Abstracta

Ano IX - N. 04

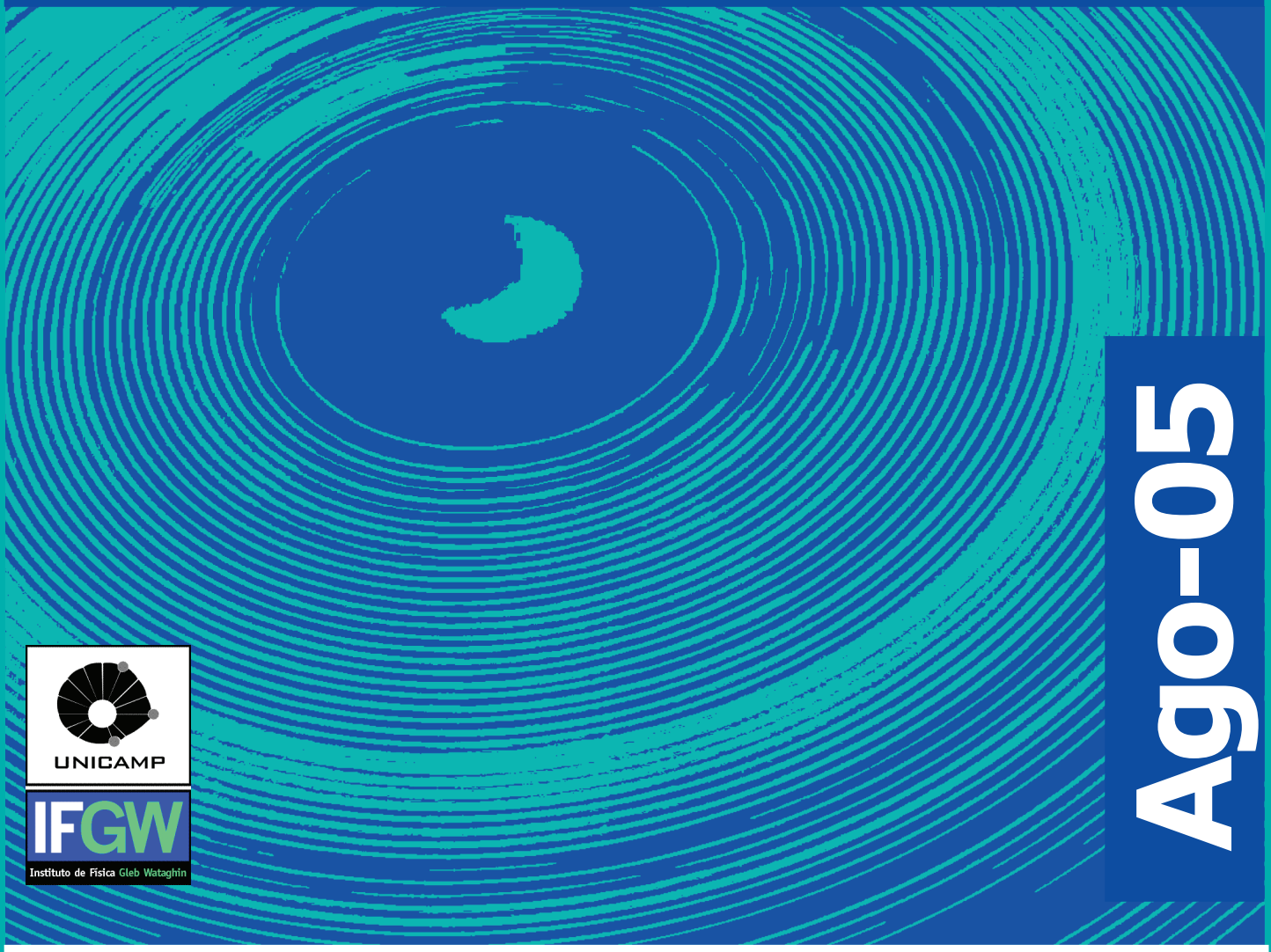

Ago-05

UNICAMP

IFGW

Instituto de Física Gleb Wataghin

Trabalhos Aceitos para Publicação

A002-05 à A006-05

Trabalhos Publicados

Junho 2005 à Julho 2005

P132-05 à P208-05

TRABALHOS ACEITOS PARA PUBLICAÇÃO

A002-05 Analysis of hydrogen production from combined photovoltaics,wind energy and secondary hydroelectricity supply in Brazil.

E.P. da Silva,A.J.Marin Neto,P. F. P. Ferreira, J. C. Camargo, F. R. Apolinário, C. S. Pinto.

In this work,the technical and economical feasibility for implementing a hypothetical electrolytic hydrogen production plant,powered by electrical energy generated by alternative renewable power sources,wind and solar,and conventional hydroelectricity,was studied mainly trough the analysis of the wind and solar energy potentials for the northeast of Brazil.The hydrogen produced would be exported to countries which do not presently have signi .cant renewable energy sources,but are willing to introduce those sources in their energy system.Hydrogen production was evaluated to be around 56.26 ·106 m3H2 /yr at a cost of 10.3 US$/kg.

Solar Energy 78[5]. 670-677. 2005

A003-05 Non-Linear Transport Properties of III-Nitrides in Electric Field.

Cloves G. Rodrigues, Àurea R. Vasconcellos, Roberto Luzzi, Valder N. Freire

We consider transport properties of polar direct-gap semiconductors in electric field, specializing the numerical calculation of the general theory to the case of n- doped III-Nitrides, in particular GaN, AIN, and InN. The nonequilibrium thermodynamic state of these materials-characterized by the variables so-called quasitemperature, quasi-chemical potential, and drift velocity of the carriers, and the quasitemperatures of LO and AC phonons- is studied. The evolution equations of these variables- which are highly nonlinear - are derived, and the transient regime and the ensuing steady state are analyzed. The nonlinear transport is characterized and its main properties are discussed. In one case comparison with a recent Monte Carlo calculation is made and a good agreement is obtained. in this paper we mainly consider the ultrafast transient, and in the following, paper the steady state.

Journal of Apllied Physics 98[4]. 043702-043702-9. 2005.

A004-05 Nonlinear Transport Properties of Doped III-N and GaAs Polar Semiconductor: a Comparison.

Clóves G. Rodrigues, Áurea R. Vasconcellos, Roberto Luzzi, Valder N. Freire.

In the previous article we have presented a study of transport properties of doped direct-gap inverted-band polar semiconductors III-Nitrides and GaAs in the steady state, calculated with a nonlinear quantum transport theory based on a nonequilibrium ensemble formalism.In the present one such results are compared with calculations using Monte Carlo-modeling simulations and with experimental measurements. Materials of the n-type and p-type doping in the presence of intermediate to high electric fields, and for several temperatures of the external reservoir, are considered. The agreement between the results obtained using the nonliear quantum kinetic theory, with those of Monte Carlo calculations and experimental data is remarkably good , thus satisfactorily validating this powerful, concise, and physically sound formalism.

Journal of Applied Physics 98[4]. 043703-043703-5. 2005.

A005-05 Ultrafast Relaxation Kinetics of Photoinjected Plasma in III-Nitrides.

Clóves G. Rodrigues, Áurea R. Vasconcellos, Roberto Luzzi

The ultrafast relaxation kinetics of the photoinjected palsma in blue-emitting highly-polar III-Nitrides is analyzed. The evolution of the nonequilibrium thermodynamic state of the “ hot carriers`` and “ hot phonons`` is studied. It is shown that the dissipative phenomena are orders of magnitude larger than in lesser polar materials, as GaAs. Moreover, the phenomena of “phonon bottleneck” and “hot-phonon temperature overshoot” are characteristically enhanced.

Journal of Physics D: Solid State 38[19]. 3584-3589. 2005.

A006-05 Influence of a dynamical gluon mass in the pp and $p^{-}p$ forward scattering.

E. G. S. Luna, A. F. Martini, J. J. Menon, A. Mihara , and A. A. Natale.

We compute the tree level cross section for gluon-gluon elastic scattering taking into account a dynamical gluon mass, and show that this mass scale is a natural regulator for this subprocess cross section. Using an eikonal approach in order to examine the relationship between this gluon-gluon scattering and the elastic pp and pp channels, we found that the dynamical gluon mass is of the same order of magnitude as the ad hoc infrared mass scale mo underlying eikonalized QCD-inspired models. We argue that this correspondence is not an accidental result, and that this dynamical scale indeed represents the onset of non-perturbative contributions to the elastic hadron-hadron scattering. We apply the eikonal model with a dynamical infrared mass scale to obtain predictions for s?totpp,pp , rpp,pp , slope B pp,pp, and differential elastic scattering cross section ds pp / dt at Tevatron and CERN-LHC energies.

Physical Review D 72[3]. 034019. 2005.

TRABALHOS PUBLICADOS

P132-05 “1D photonic band gap PbTe doped silica quantum dot optical device”.

Rodriguez, E., Jimenez, E., Cesar, C. L., Barbosa, L. C., and de Araujo, C. B.

Thin films of glass doped with PbTe quantum dots (QDs) were successfully fabricated The semiconducting nanocrystallites were grown by laser ablation of a PbTe target (99.99%) using the second harmonic of a Q-Switched Quantel Nd: YAG laser under a high purity argon atmosphere. The glass matrix was fabricated by a plasma chemical vapour deposition method using tetramethoxysilane (TMOS) vapour as precursor The QDs and the glass matrix were alternately deposited onto a Si (100) wafer for 60 cycles. A cross sectional TEM image clearly showed the QD layers well separated from each other by glass matrix layers. The influence of the ablation time and the laser fluence on the density and size distribution of the quantum dots was studied. HRTEM revealed anisotropy in the size of the QDs: they were about 9 nm in height and 3-5 nm in diameter Furthermore HRTEM studies revealed that the QDs basically grew in the (200) and (220) directions. The thickness of the glass matrix layer was about 20 nm. Absorption, photoluminescence and nonlinear optical properties of the device are currently being measured

Glass Technology - European Journal of Glass Science and Technology Part A 46[2]. 47-49. 2005.

P133-05 "Ab initio two-body potentials and the properties of condensed phases of helium atoms".

Ujevic, S. and Vitiello, S. A.

A careful comparison of some properties of systems of helium atoms in the liquid and solid phases is performed for several ab initio two-body potentials from the literature. Additional contributions from a three-body potential are considered as well. The multiweight diffusion Monte Carlo method is employed to quantitatively compute the small changes in the properties of the system as the different potentials are considered.

Physical Review B 71[22]. 224518. 2005.

P134-05 "Address by the President of the Organizing Committee".

Hadler, J. C.

Radiation Measurements 39[6], 575-576. 2005.

P135-05 "Advances on the Brazilian toroidal grating monochromator (TGM) beamline".

Cavasso, R. L., Homem, H. G. P., Landers, R., and de Brito, A. N.

We report on an important advance for the vacuum ultraviolet and soft X-ray TGM beamline at Laboratorio Nacional de Luz Sincrotron (LNLS). This beamline provides photons in the energy range 12-330 eV using three gratings. It is well known that TGMs deliver relatively high flux at these energies but harmonic contamination can be a serious problem. Of special interest for the users is the range between 12 and 21 eV covered by one of the gratings for studies of outer and inner valence ionization processes in gases as well as solids. Here, we report a solution to the harmonic contamination problems based on a noble gas phase filter combined with thin metal foil barriers.

Journal of Electron Spectroscopy and Related Phenomena 144-147, 1125-1127. 2005.

P136-05 "Alpha-particle calibration of CR-39 using a beehive collimator".

Santos, N. F., Neto, J. C. H., Iunes, P. J., Guedes, S., and Paulo, S. R.

A device to determine the detection efficiency of CR-39 for alpha particles is presented. A beehive collimator restricted the angle of incidence of alpha particles on a CR-39 sheet, such that the total number of alpha emitters could be determined. This makes it possible to obtain the critical angle of incidence, Theta(C), and the maximum angle of incidence resulting in round (diameter ratio < 1.100) etch pits, Theta(max). In this work, these angles were determined for incidence energies around 7.5 MeV (more specifically 6.1 and 8.8 MeV).

Radiation Measurements 39[6], 661-664. 2005.

P137-05 "Annealing crystallization of a-Ge/Al/Si and a-Ge/Si thin films".

Fajardo, F., Zanatta, A. R., and Chambouleyron, I.

This work describes the temperature-induced crystallization of amorphous Ge (a-Ge) as a function of the thickness of the a-Ge films (in the 12-2600 nm range), which were deposited both onto c-Si substrates and c-Si substrates covered with aluminium. After deposition, the samples were submitted to cumulative thermal annealing treatments. It is shown that the temperature of crystallization depends on the thickness of the a-Ge films and to the presence (or not) of the Al layer. For an annealing temperature (T-a) of similar to 700 degrees C, for example, the Raman spectra of films thinner than similar to 1000 nm and deposited onto c-Si substrates are completely dominated by the sharp phonon mode of crystalline Si. Films with thicknesses equal to 300, 1000 and 2600 nm, deposited onto Al/c-Si, and treated at T-a = 600 degrees C, on the other hand, clearly display two additional peaks at 405 and 490 cm(-1). They correspond to the Raman modes of Si-Ge and Si-Si modes, suggesting the formation of a SiGe alloy during the thermal anneal of the films.

Physica Status Solidi B-Basic Solid State Physics 242[9], 1906-1909. 2005.

P138-05 "Avoided antiferromagnetic order and QCP in CeCoIn5".

Bianchi, A., Movshovich, R., Vekhter, I., Pagliuso, P. G., and Sarrao, J. L.

We measured the specific heat and resistivity of heavy fermion CeCoIn5 between the superconducting critical field H-c2, = 4.95 and 9T, with the field in the [001] direction, and at temperatures down to 50mK. These results show that this compound has a quantum critical point (QCP) with the magnetic field as the tuning parameter. For a field of 5 T just above H-c2 the temperature dependence of both specific heat C-p(T) and resistivity rho(T) show non-Fermi liquid (NFL) behavior down to the lowest temperatures with C-p(T) alpha - log(T) and rho(T) - rho(T = 0) alpha T. For fields above 8 T the data exhibit a crossover from a NFL to a Fermi liquid behavior. Specific heat and resistivity data show behavior predicted by spin-fluctuation theory, suggesting that the NFL behavior is due to incipient antifierromagnetism (AFM) in CeCoIn5 with the quantum critical point in the vicinity of H-c2. For fields below H-c2 the AFM phase separated by a QCP from the paramagnetic ground state is not observed, as the system becomes first superconducting.

Physica B-Condensed Matter 359, 74-76. 2005.

P139-05 "Bundling up carbon nanotubes through Wigner defects".

da Silva, A. J. R., Fazzio, A., and Antonelli, A.

We show, using ab initio total energy density functional theory, that the so-called Wigner defects, an interstitial carbon atom right beside a vacancy, which are present in irradiated graphite, can also exist in bundles of carbon nanotubes. Due to the geometrical structure of a nanotube, however, this defect has a rather low formation energy, lower than the vacancy itself, suggesting that it may be one of the most important defects that are created after electron or ion irradiation. Moreover, they form a strong link between the nanotubes in bundles, increasing their shear modulus by a sizable amount, clearly indicating its importance for the mechanical properties of nanotube bundles.

Nano Letters 5[6], 1045-1049. 2005.

P140-05 "Characterization of human skin through photoacoustic spectroscopy".

Rompel, P. C. B., dos Anjos, F. H., Mansanares, A. M., da Silva, E. C., Acosta-Avalos, D., and Barja, P. R.

The photoacoustic (PA) technique is based on the absorption of modulated or pulsed light by a sample with subsequent heat generation, generating thermal waves that propagate in the surrounding media.

Such waves produce the pressure oscillation detected as the PA signal. In this work, PA spectroscopy was used to characterize different human skin samples with respect to their response to ultraviolet radiation (UVA and UVB, 240nm < lambda < 400nm). Measurements were performed at 70Hz and 17Hz, using a 1000W Xe arc lamp as the light source. Skin samples were about 0,5cm diameter. It was possible to obtain the absorption spectra of the stratum corneum and of a deeper layer of epidermis; when the lower modulation frequency is utilized, PA spectroscopy characterizes the absorption of the whole epidermis, because in this case the thermal diffusion length is thicker than that of the stratum corneum. PA spectroscopy was also employed to monitor the drying kinetics of the skin. Pre-treatment of the samples included different periods in a drying chamber. Measurements show that the PA spectra changes according to the humidity of the skin. Future work includes detailed monitoring of skin hydration

Journal de Physique IV (Proceedings) 125[1], 785-787. 2005.

P141-05 "Charge buildup effects in asymmetric p-type resonant tunneling diodes".

Gobato, Y. G., Brasil, M. J. S. P., Camps, I., de Carvalho, H. B., dos Santos, L. F., Marques, G. E., Henini, M., Eaves, L., and Hill, G.

We have investigated p-doped GaAs-AlAs resonant tunneling devices with asymmetric barriers under optical excitation. Transport and photo luminescence measurements were performed under identical bias conditions as a function of the light excitation intensity. We have observed the development of additional peaks, induced by illumination, between the main light- and heavy-hole resonances in the current-voltage characteristics (I(V)). We describe the behavior of these photo-induced peaks under a magnetic field parallel to the current. We propose that the observed properties are related to resonant tunneling of photoinduced electrons and associated excitonic effects.

Microelectronics Journal 36[3-6], 356-358. 2005.

P142-05 "Coherent-state superpositions in cavity quantum electrodynamics with trapped ions".

Semiao, F. L. and Vidiella-Barranco, A.

We investigate how superpositions of motional coherent states naturally arise in the dynamics of a two-level trapped ion coupled to the quantized field inside a cavity. We extend our considerations, including a more realistic setup where the cavity is not ideal and photons may leak through its mirrors. We found that a detection of a photon outside the cavity would leave the ion in a pure state. The statistics of the ionic state still keeps some interference effects that might be observed in the weak-coupling regime.

Physical Review A 71[6]. 065802. 2005.

P143-05 "Crystal structure and low-temperature physical properties of R3M4Sn13 (R = Ce, La; M = Ir, Co) intermetallics".

Israel, C., Bittar, E. M., Aguero, O. E., Urbano, R. R., Rettori, C., Torriani, I., Pagliuso, P. G., Moreno, N. O., Thompson, J. D., Hundley, M. F., Sarrao, J. L., and Borges, H. A.

We have synthesized single crystalline samples of R3M4Sn13 (R = Ce, La; M = Ir, Co) using a Sn-flux method. Measurements of magnetic susceptibility and heat capacity indicate heavy-fermion behavior for the Ce-based compounds. The crystal structure of these intermetallic compounds has been determined by Rietveld refinement from X-ray powder diffraction data. They crystallize in a Yb3M4Sn13 type structure (Pm-3n), which has 40 atoms per unit cell. The low-temperature physical properties of these intermetallic compounds are reported.

Physica B-Condensed Matter 359, 251-253. 2005.

P144-05 "Dipolar interaction and size effects in powder samples of colloidal iron oxide nanoparticles".

Vargas, J. M., Socolovsky, L. M., Knobel, M., and Zanchet, D.

Dipole-dipole interactions in nanostructured materials deeply affect their magnetic properties, and detailed studies are still required to fully understand them. In this work, the dependence of magnetic properties on particle size has been evaluated in powder samples of Fe oxide nanoparticles produced by colloidal methods. Zero-field-cooled and field-cooled magnetization curves and magnetization versus applied field data have been analysed by taking into account dipolar interactions through a correction to the classical superparamagnetic model. Morphological and magnetic data were in very good agreement, which has allowed us to quantify relevant physical parameters, such as the anisotropy constant, magnetic moment, and interacting volume for our system.

Nanotechnology 16[5], S285-S290. 2005.

P145-05 "Effects of applied magnetic fields on direct and indirect excitons in coupled semiconductor quantum wells".

Reyes-Gomez, E., Oliveira, L. E., and Dios-Leyva, M.

We have investigated magnetic-field effects on the direct- and indirect-exciton dispersions and on the exciton effective mass in the plane perpendicular to the applied field, within the variational framework and effective-mass approximation, for coupled GaAs-(Ga,Al)As quantum wells. The simple hydrogen-like envelope wave function we have used provides the expected behavior for the exciton dispersion law in a wide range of the center-of-mass momenta, and leads to an analytical expression for the exciton effective mass. Theoretical results for the magnetic-field dependent exciton dispersion and effective mass are in quite good agreement with available experimental measurements.

Physica Status Solidi B-Basic Solid State Physics 242[9], 1829-1832. 2005.

P146-05 "Effects of applying stress on the electron field emission properties in amorphous carbon thin films".

Poa, C. H. P., Silva, S. R. P., Lacerda, R. G., Amaratunga, G. A. J., Milne, W. I., and Marques, F. C.

Diamond-like carbon (DLC) films have always had high intrinsic stress due to their metastable structure and the fine balance between film density and bond stability. We show the effects of high intrinsic stress on the electron field emission performance, where a lower electric field for emission is recorded with increasing stress in the DLC films. In addition to examining "as deposited" films with different magnitudes of intrinsic stress, we subject the DLC films to external pressure by physically bending the a-C/silicon substrates. The result is a phenomenon where electrons are "squeezed" out of the films, and can be applied to the fabrication of stress sensors.

Applied Physics Letters 86[23]. 232102. 2005.

P147-05 "Effects of dipolar interactions on magnetic properties of granular solids".

Brandl, A. L., Socolovsky, L. M., Denardin, J. C., and Knobel, M.

The magnetic behavior of superparamagnetic Co nanoparticles (2-4 nm in diameter) dispersed in an amorphous, insulating SiO2 matrix was studied.

Conventional fittings of magnetization curves present mean magnetic moments which diminish with decrease in temperature. In order to treat this anomalous behavior, we have applied the interacting superparamagnetic model (ISP). Mean diameters obtained from transmission electron microscopy (TEM) were compared with values obtained applying ISP model.

Journal of Magnetism and Magnetic Materials 294[2], 127-132. 2005.

P148-05 "Electron-hole transitions in self-assembled InAs/GaAs quantum dots: Effects of applied magnetic fields and hydrostatic pressure".

Duque, C. A., Porras-Montenegro, N., Barticevic, Z., Pacheco, A., and Oliveira, L. E.

A theoretical study of the effects of applied magnetic fields and hydrostatic pressure on the electron-hole transition energies in self-assembled InAs/GaAs quantum dots is presented. The effective-mass approximation and a model of a cylindrical-shaped quantum dot with in-plane parabolic potential have been used to describe the InAs/GaAs quantum dots. Present theoretical results are in quite good agreement with experimental measurements of the magnetic field and pressure dependence of the exciton transition energies in InAs/GaAs self-assembled quantum dots.

Microelectronics Journal 36[3-6], 231-233. 2005.

P149-05 "Entanglement dynamics for two interacting spins".

Novaes, M.

We study the dynamical generation of entanglement for a very simple system: a pair of interacting spins, s(1) and s(2), in a constant magnetic field. Two different situations are considered: (a) s(1) -> infinity, s(2) = 1/2 and (b) s(1) = s(2) -> infinity, corresponding, respectively, to a quantum degree of freedom coupled to a semiclassical one (a qubit in contact with an environment) and a fully semiclassical system, which in this case displays chaotic behavior. Relations between quantum entanglement and classical dynamics are investigated.

Annals of Physics 318[2], 308-315. 2005.

P150-05 "Evolution from insulator (x=0.003) to metal (x=1) of the Eu2+ local environment in Ca1-xEuxB6".

Urbano, R. R., Pagliuso, P. G., Rettori, C., Schlottmann, P., Nakatsuji, S., Fisk, Z., Sarrao, J. L., Bianchi, A., and Oseroff, S. B.

The local environment of Eu2+ (4f(7) S=7/2) in Ca1-xEuxB6 (0.003 <= x <= 1.00) is studied by means of electron spin resonance (ESR). For x less than or similar to 0.07 the resonances have Lorentzian line shape, indicating an insulating environment for the Eu2+ ions. For x greater than or similar to 0.07, the lines broaden and become Dysonian in shape, suggesting a change to metallic environment for the EU2+, ions, anticipating the semimetallic character of EuB6. The broadening is attributed to a spin-flip scattering relaxation process due to the exchange interaction between conduction and Eu(2+)4f electrons. High field ESR measurements for x greater than or similar to 0.30 reveal narrower and anisotropic linewidths, which are attributed to magnetic polarons and Fermi surface effects, respectively.

Journal of Applied Physics 97[10]. 10A924. 2005.

P151-05 "Fission-track dating of South American natural glasses: an overview".

Bigazzi, G., Neto, J. C. H., Iunes, P. J., and Araya, A. M. O.

Although many glass-bearing horizons can be found in South American volcanic complexes or sedimentary series, only a relatively few tephra and obsidian-bearing volcanic fields have been studied using the fission-track (FT) dating method. Among them, the volcanics located in the Sierra de Guamani (east of Quito, Ecuador) were studied by several authors. Based upon their ages, obsidians group into three clusters: (1) very young obsidians, similar to 0.2Ma old, (2) intermediate-age obsidians, similar to 0.4- similar to 0.8 Ma old, and (3) older obsidians, similar to 1.4- similar to 1.6 Ma old. The FT method is also an efficient alternative technique for identification of the sources of prehistoric obsidian artefacts. Provenance studies carried out in South America have shown that the Sierra de Guamani obsidian occurrences were important sources of raw material for toot making during pre-Columbian times. Glasses originated from these sources were identified in sites distributed over relatively wide areas of Ecuador and Colombia. Only a few systematic studies on obsidians in other sectors were carried out. Nevertheless, very singular glasses have been recognised in South America, such as Macusanite (Peru) and obsidian Quiron (Argentina), which are being proposed as additional reference materials for FT dating. Analyses of tephra beds interstratified with sedimentary deposits revealed the performance of FT dating in tephrochronological studies. A remarkable example is the famous deposit outcropping at Farola Monte Hermoso, near Bahia Blanca (Buenos Aires Province), described for the first time by the middle of the 19th century by Charles Darwin. Considering the large number of volcanic glasses that were recognised in volcanic complexes and in sedimentary series, South America is a very promising region for the application of FT dating. The examples given above show that this technique may yield important results in different disciplinary fields.

Radiation Measurements 39[6], 585-594. 2005.

P152-05 "Fluorescence quantum efficiency of Er3+ in low silica calcium aluminate glasses determined by mode-mismatched thermal lens spectrometry".

Sampaio, J. A., Gama, S., Baesso, M. L., and Catunda, T.

The fluorescence quantum efficiency of Er3+ in low silica calcium aluminate glasses, with nominal composition 58 CaO, 27.1 - x Al2O3, 6.9 MgO, 8 SiO2, x Er2O3, 0.1 <= X <= 1.5 (mol%), melted in air and under vacuum, has been measured using the mode-mismatched thermal lens spectrometry, with excitation beam wavelength at 488 nm and 804 nm. From 0.1 up to 1.1 mol% of Er2O3 the quantum efficiency is around 0.65 for vacuum-melted samples, and around 0.46 for air-melted ones. The quenching of the quantum efficiency appears above 1.3 mol% of Er2O3. The thermal diffusivity was also obtained, with results showing a decrease from 5.69 x 10(-3) cm(2)/s (undoped sample) to 4.78 x 10-3 cm(2)/s (for the highest doped sample, 1.5 mol% of Er2O3).

Journal of Non-Crystalline Solids 351[19-20], 1594-1602. 2005.

P153-05 "Gapless-excitation induced resistivity in ferromagnetic layers".

Ferrer, A. V., Farinas, P. F., and Caldeira, A. O.

Magnetic domains in a two-dimensional ferromagnetic metal and the existence of gapless magnons confined along the domain walls are studied starting from the XXZ model for localized spins. The relevance for transport properties of the inelastic interaction between conduction electrons and the localized magnons is analysed, and conductivity calculations presented.

Philosophical Magazine 85[20], 2293-2322. 2005.

P154-05 "Gradual transition from insulator to semimetal of Ca1-xEuxB6 with increasing Eu concentration".

Urbano, R. R., Pagliuso, P. G., Rettori, C., Schlottmann, P., Sarrao, J. L., Bianchi, A., Nakatsuji, S., Fisk, Z., Velazquez, E., and Oseroff, S. B.

The local environment of Eu2+ (4f(7),S=7/2) in Ca1-xEuxB6 ((.003 <= x <= 1.00) is investigated by means of electron spin resonance (ESR). For x less than or similar to 0.003 the spectra show resolved fine and hyperfine structures due to the cubic crystal electric field and nuclear hyperfine field, respectively. The resonances have Lorentzian line shape, indicating an insulating environment for the Eu2+ ions. For 0.013 less than or similar to x less than or similar to 0.07, as x increases, the ESR lines broaden due to local distortions caused by the Eu/Ca ions substitution. For 0.07 less than or similar to x less than or similar to 0.30, the lines broaden further and the spectra gradually change from Lorentzian to Dysonian resonances, suggesting a coexistence of both insulating and metallic environments for the Eu2+ ions. In contrast to Ca1-xGdxB6, the fine structure is still observable up to x approximate to 0.15. For x greater than or similar to 0.30 the fine and hyperfine structures are no longer observed, the line width increases, and the line shape is purely Dysonian, anticipating the semimetallic character of EuB6. This broadening is attributed to a spin-flip scattering relaxation process due to the exchange interaction between conduction and Eu2+ 4f electrons. High-field ESR measurements for x greater than or similar to 0. 5 reveal smaller and anisotropic linewidths, which are attributed to magnetic polarons and Fermi surface effects, respectively.

Physical Review B 71[18]. 184422. 2005.

P155-05 "Ground state phases of the two-leg Kondo ladder".

Xavier, J. C. and Miranda, E.

We present the ground state phase diagram of the two-leg Kondo ladder obtained through the density-matrix renormalization group. At half-filling, the spin and charge gaps are non-zero. At other conduction electron densities, we have found fully and partially saturated ferromagnetism, paramagnetism, and dimerized phases at special commensurate fillings.

Physica B-Condensed Matter 359-361, 102-104. 2005.

P156-05 "Hidden consequence of active local Lorentz invariance".

Rodrigues, W. A., Da Rocha, R., and Vaz, J.

In this paper we investigate a hidden consequence of the hypothesis that Lagrangians and field equations must be invariant under active local Lorentz transformations. We show that this hypothesis implies in an equivalence between spacetime structures with several curvature and torsion possibilities.

International Journal of Geometric Methods in Modern Physics 2[2], 305-357. 2005.

P157-05 "Hidden order in CeMIn5".

Thompson, J. D., Balatsky, A. V., Nicklas, M., Pagliuso, P. G., Sarrao, J. L., and Sidorov, V. A.

Experiments suggest that some form of hidden order, possibly related to field-induced transitions, may be important for superconductivity in CeIrn(5) at atmospheric pressure and in the very high-pressure phase of CeRhIn5.

Physica B-Condensed Matter 359, 392-394. 2005.

P158-05 "Imaging and switching of Fano resonances in open quantum cavities".

Mendoza, M. and Schulz, P. A.

We present a systematic numerical investigation of the imaging of states in highly transmiting open quantum dots within a Green's function method applied to a tight-binding lattice model. We show evidence that images obtained from conductance change are not bona fide images of the unperturbed probability densities, because the coupled quantum dot-tip system induces coupling between several resonances, hindering a reliable interpretation of the conductance maps. We suggest that mapping the energy shifts of the resonances may provide the necessary complementary tool for good wave function imaging in quantum billiards.

Physical Review B 71[24]. 245303. 2005.

P159-05 "In situ photoemission electron spectroscopy of plasma-nitrided metal alloys".

Figueroa, C. A. and Alvarez, F.

In this paper, we report the influence of oxygen on the structure and chemical compositions of the surface of low-energy (similar to 50 eV) implanted stainless steel studied by in situ photoemission electron spectroscopy. The presence of oxygen at the surface forms thermodynamically stable oxides and hydroxides, degrading metallic nitrides, and preventing efficient nitrogen diffusion into the bulk material. Among these metallic nitrides, gamma(N) and FeNx are more susceptible to oxidize. Lower oxygen partial pressures augment nitrogen content at the surface determining material bulk properties.

Journal of Applied Physics 97[10]. 103528. 2005.

P160-05 "Kinetic model for the relationship between mean diameter shortening and age reduction in glass samples".

Guedes, S., Iunes, P. J., Hadler, J. C., Bigazzi, G., Tello, C. A. S., Alencar, I., Palissari, R., Curvo, E. A. C., and Moreira, P. A. F. P.

Fission tracks in glass samples are shortened when they experience thermal treatment. Consequently, the observable dimensions associated with track length also diminish. The dimension normally used to characterize track size is the mean diameter of the etched track at the surface, D. Another consequence of length shortening is the reduction of surface density, p, implying a reduction of the fission-track age. In this work, a kinetic model is developed to describe the relationship between fission-track mean diameter shortening and surface fission-track density reduction in glass samples, based on geometrical and etching hypotheses. The result is a two-parameter equation given by rho/rho(0) = (D/D-0)(2(1+1/n)) (4h(2) + D-0(2)/4h(2)+D-0(2)(D/D-0)(2))(2) (4h(2) - D-0(2)/4h(2)-D-0(2)(D/D-0)(2))(1/n) (1) in which h is the thickness of the layer removed during etching and n is a parameter related to the latent track geometry and etching reaction rate. The equation was compared with experimental data on Australite glass found in the literature and with fresh data on Macusanite glass presented in this work. The model fits the experimental curves quite well, showing that it describes the etching effects correctly (within its limitations). In addition, the model equation derived in this work can be very useful in age correction of partially annealed glass samples.

Radiation Measurements 39[6], 647-652. 2005.

P161-05 "Magnetization and specific heat in U1-xLaxGa2 and magnetocaloric effect in UGa2".

da Silva, L. M., Gandra, F. G., Medina, A. N., dos Santos, A. O., and Cardoso, L. P.

We have investigated the properties of the ferromagnetic series U1-xLaxGa2. The magnetization results show a reduction of mu(eff) and of T-c when x is increased. The electronic coefficient gamma of the specific heat increases to a maximum of 260 mJ/Umol K-2 at x=0.75. This behavior is probably consequence of delocalization of 5f electrons, causing enhancement of the density of states. For x=0.9 the ordering disappears and a non-Fermi-liquid behavior is observed. UGa2 also presented a significant magnetocaloric effect of Delta S-mag=-3.5 J/kg K at 120 K and H=7 T which can be modified by chemical pressure.

Journal of Applied Physics 97[10]. 10A921-10A921-3. 2005.

P162-05 "Magnetocaloric effect of La0.8Sr0.2MnO3 compound under pressure".

Rocco, D. L., Silva, R. A., Magnus, A., Carvalho, G., Coelho, A. A., Andreeta, J. P., and Gama, S.

The La0.8Sr0.2MnO3 compound presents a ferromagnetic paramagnetic transition around room temperature to which a reasonably high magnetocaloric effect is associated, turning this material of interest for application in magnetic refrigeration. We synthesized this compound in fiber single crystalline form by the Laser Heated Pedestal Growth method. The sample was characterized by x-ray diffraction and magnetic measurements as a single phase and with the required magnetic properties. We measured the magnetic properties and the magnetocaloric effect under hydrostatic pressure for pressures up to 6 kbar as a function of temperature. Our results indicate that the Curie temperature increases with pressure while the low temperature transition from the orthorhombic to the rhombhoedral structures decreases as pressure increases. This is in close agreement with the literature. Measurement of the magnetocaloric effect at the high temperature transition indicates that the peak of the effect follows the trend of the Curie temperature, but its maximum value remains almost constant as a function of pressure.

Journal of Applied Physics 97[10]. 10M317-10M317-3. 2005.

P163-05 "Mechanism of lateral ordering of InP dots grown on InGaP layers".

Bortoleto, J. R. R., Gutierrez, H. R., Cotta, M. A., and Bettini, J.

The mechanisms leading to the spontaneous formation of a two-dimensional array of InP/InGaP dots grown by chemical-beam epitaxy are discussed. Samples where the InGaP buffer layer was grown at different conditions were characterized by transmission electron microscopy.Our results indicate that a periodic strain field related to lateral two-dimensional compositional modulation in the InGaP buffer layer determines the dot nucleation positions during InP growth. Although the periodic strain field in the InGaP is large enough to align the InP dots, both their shape and optical properties are effectively unaltered. This result shows that compositional modulation can be used as a tool for in situ dot positioning.

Applied Physics Letters 87[1]. 013105. 2005.

P164-05 "Motion of a particle with isospin in the presence of a monopole".

Fernandes, R. M. and Letelier, P. S.

From a consistent expression for the quadriforce describing the interaction between a colored particle and gauge fields, we investigate the relativistic motion of a particle with isospin interacting with a BPS monopole and with a Julia-Zee dyon. The analysis of such systems reveals the existence of unidimensional unbounded motion and asymptotic trajectories restricted to conical surfaces, which resembles the equivalent case of electromagnetism.

Physics Letters A 341[1-4], 22-32. 2005.

P165-05 "Nodal liquid and s-wave superconductivity in transition metal dichalcogenides".

Uchoa, B., Cabrera, G. G., and Neto, A. H. C.

We explore the physical properties of a unified microscopic theory for the coexistence of superconductivity and charge-density waves (CDWs) in two-dimensional transition-metal dichalcogenides. In the case of particle-hole symmetry, the elementary particles are Dirac fermions at the nodes of the charge density wave gap. When particle-hole symmetry is broken, electron (hole) pockets are formed around the Fermi surface. The superconducting ground state emerges from the pairing of nodal quasiparticles mediated by acoustic phonons via a piezoelectric coupling. We calculate several properties in the s-wave superconducting phase, including specific heat, ultrasound absorption, nuclear magnetic relaxation (NMR), and thermal and optical conductivities. In the case with particle-hole symmetry, the specific-heat jump at the transition deviates strongly from ordinary superconductors. The NMR response shows an anomalous anisotropy due to the broken time-reversal symmetry of the superconducting gap, induced by the triple CDW state. The loss of the lattice inversion center in the CDW phase leads to anomalous coherence factors in the optical conductivity and to the appearance of an absorption edge at the optical gap energy. In addition, optical and thermal conductivities display anomalous peaks in the infrared when particle-hole symmetry is broken.

Physical Review B 71[18]. 184509. 2005.

P166-05 "Non-conditioned generation of Schrodinger cat states in a cavity".

Munhoz, P. P. and Vidiella-Barranco, A.

We investigate the dynamics of a two-level atom in a cavity filled with a nonlinear medium. We show that the atom-field detuning delta and the nonlinear parameter chi((3)) may be combined to yield a periodic dynamics, allowing the generation of almost exact superpositions of coherent states (Schroodinger cats). By analysing the atomic inversion and the field purity, we verify that any initial atom-field state is recovered at each revival time, and that a coherent field interacting with an excited atom evolves to a superposition of coherent states at each collapse time. We show that a mixed field state (statistical mixture of two coherent states) evolves towards an almost pure field state as well (Schroodinger cat). We discuss the validity of these results by using the field fidelity and the Wigner function.

Journal of Modern Optics 52[11], 1557-1573. 2005.

P167-05 "Non-linear phenomena in atoms and clusters induced by intense VUV radiation from a free electron laser".

de Castro, A. R. B., Bostedt, C., Gurtler, P., Laarmann, T., Laasch, W., Schulz, J., Swiderski, A., Wabnitz, H., and Moller, T.

We report on first experiments of rare gas cluster dynamics and spectroscopy using light from the DESY free electron laser at 13 eV. The energy absorption is found to be very efficient and the clusters fragment completely. Non-linear effects appear at a peak power density threshold much lower than for visible light.

The data are consistent with a three-step ionization process, but the nature of the first step is still controversial.

Journal of Electron Spectroscopy and Related Phenomena 144, 3-6. 2005.

P168-05 "On epidote fission track dating".

Curvo, E. A. C., Neto, J. C. H., Iunes, P. J., Guedes, S., Tello, C. A. S., Paulo, S. R., Hackspacher, P. C., Palissari, R., and Moreira, P. A. F. P.

The use of epidote in fission track dating was abandoned since the beginning of the 1980s due to difficulties like absence of a standard etching procedure, obtainment of different closure temperatures and the percentage of the datable samples. The results become much more reproducible when restricting fission track analysis to a peculiar kind of track. We are also studying confined track length, what makes possible to obtain information about fossil track annealing. Fission tracks in epidote were successfully etched with 48% HF at 35 degrees C for 12.5 min. Dating samples by the external detector method was not possible due to problems in measuring the efficiency factor held between the number of fossil fission tracks and tracks induced in mica. Dating a sample from Brejui, RN, Brazil with the population method gave a corrected age of 510 +/- 69Ma, in agreement with published U/Th-Pb ages. From the fact that the fossil track length histogram was bimodal, we were able to infer that this sample registered a thermal episode during its history. These preliminary results indicate that epidote deserves further studies to establish whether it can be employed as a thermochronological tool.

Radiation Measurements 39[6], 641-645. 2005.

P169-05 "On indoor radon daughters plate-out on material surfaces".

Neman, R., Hadler, J. C. N., Iunes, P. J., and Paulo, S. R.

In this work, the plate-out of radon daughters on surfaces of different sizes has been studied. Several pieces of CR-39, cut circularly with different diameters, were exposed for approximately 3 months in an indoor environment containing a high concentration of uranium in Pocos de Caldas, Brazil. During the exposition the CR-39 sheets remained fixed in a wire far from any object. After the exposition, the etched alpha tracks were counted and mapped in order to obtain the spatial distribution of tracks on the detector surface. The accomplished experimental results are in agreement with the theoretical and computational conclusions obtained in previous works.

Radiation Measurements 39[6], 653-655. 2005.

P170-05 "Optical configurations for pump and probe experiments with a VUV free-electron laser".

de Castro, A. R. B. and Moller, T.

We discuss strategies for color separation and recombination, regarding 2-color pump-and-probe experiments planned for the DESY XUV FEL Phase 2. We show that efficient handling of the pump and probe components, with good spectral and spatial separation, is possible with either filters or gratings; the former are cheap while the latter are continuously tunable over a range. Nice spatial overlap of the pump and probe on a spot 5 x 8 mu m(2) FWHM, limited by surface slope errors on the optics, can be achieved with a Kirkpatrick-Baez pair of cylindrical elliptic mirrors placed about 500 mm away from the sample position. Thermal loading is also discussed. It is found that the filters cannot survive more than a few dozen FEL pulses in a train, while a grating on a water-cooled silicon thin blade will present unacceptable surface slope errors after about 1800 FEL pulses on a train.

Nuclear Instruments & Methods in Physics Research Section A-Accelerators Spectrometers Detectors and Associated Equipment 545[3], 568-577. 2005.

P171-05 "Perturbing the superconducting planes in CeCoIn5 by Sn substitution".

Daniel, M., Bauer, E. D., Han, S. W., Booth, C. H., Cornelius, A. L., Pagliuso, P. G., and Sarrao, J. L.

In contrast to substitution on the Co or Ce site, Sn substitution has a remarkably strong effect on superconductivity in CeCoIn5-xSnx, with T-c-> 0 beyond only similar to 3.6% Sn. Instead of being randomly distributed on in-plane and out-of-plane In sites, extended x-ray absorption fine structure measurements show the Sn atoms preferentially substitute within the Ce-In plane. This result highlights the importance of the In(1) site to impurity scattering and clearly demonstrates the two-dimensional nature of superconductivity in CeCoIn5

Physical Review Letters 95[1]. 016406. 2005.

P172-05 "Photo acoustic study of plants exposed to varying light intensity growth conditions: Spectral and morphological changes".

Mesquita, R. C., Barja, P. R., da Silva, E. C., and Mansanares, A. M.

In this paper we describe results of photo acoustic (PA) measurements carried out on various plants exposed to varying light intensity conditions. Depending on the species and light intensity conditions, the PA absorption spectra show differences in peaks associated with pigments and the cuticle. These differences are related to the spatial distribution of the pigments that differs from plant to plant. We have also performed systematic study of oxygen evolution at different wavelengths. The obtained oxygen spectra are equivalent to the action spectra usually acquired by determining the CO2 uptake and energy storage. The intensities of oxygen spectra exhibit differences depending on distinct morphology of plant

Journal de Physique IV (Proceedings) 125[1], 745-748. 2005.

P173-05 "Photoluminescence and relaxation processes in MEH-PPV".

Cossiello, R. F., Kowalski, E., Rodrigues, P. C., Akcelrud, L., Bloise, A. C., DeAzevedo, E. R., Bonagamba, T. J., and Atvars, T. D. Z.

A detailed description of the thermal relaxation processes in MEH-PPV is reported. Bulk methods such as DMTA were employed in conjunction with other techniques that probe molecular motions. such as fluorescence spectroscopy, thermal stimulated current. and C-13 NMR. From the two main transitions observed (glass transition process at 340 K and beta-relaxation between 200 and 220 K). it was demonstrated that the first is strongly correlated with the dissociation of a fluorescent emissive interchain complex and that the second relaxation involves movements of the lateral substituents of the polymer backbone and, more specifically, their CH2 groups. NMR dipolar chemical shift correlation experiments pointed an increasing gain in mobility through the side chain. the lateral carbons close to the aromatic ring being more rigid than those located more distant from be main polymer chain. A kinetic model involving the dissociation of interchains to re-form intrachain excitons was proposed to explain the profiles of the photolumineseence spectra at higher temperatures

Macromolecules 38[3], 925-932. 2005.

P174-05 "Photoluminescence spectrum of an interacting two-dimensional electron gas at nu=1".

Doretto, R. L. and Caldeira, A. O.

We report on the theoretical photoluminescence spectrum of an interacting two-dimensional electron gas at filling factor one (nu=1). We considered a model similar to the one adopted to study the x-ray spectra of metals and solved it analytically using the bosonization method previously developed for the two-dimensional electron gas at nu=1. We calculated the emission spectra of the right and the left circularly polarized radiations for the situations where the distance between the two-dimensional electron gas and the valence band hole is smaller and greater than the magnetic length. For the former, we showed that the polarized photoluminescence spectra can be understood as the recombination of the so-called excitonic state with the valence band hole whereas, for the latter, the observed emission spectra can be related to the recombination of a state formed by a spin down electron bound to n spin waves. This state seems to be a good description for the quantum Hall skyrmion.

Physical Review B 71[24]. 245330. 2005.

P175-05 "Photothermal methods and atomic force microscopy images applied to the study of poly(3-hydroxybutyrate) and poly(3-hydroxybutyrate-co-3-hydroxyvalerate) dense membranes".

Poley, L. H., Siqueira, A. P. L., da Silva, M. G., Sanchez, R., Prioli, R., Mansanares, A. M., and Vargas, H.

Thermal and transport properties of some polyhydroxyalkanoates (PHAs), poly-3- hydroxybutyrate and poly-3-hydroxybutyrate-co-3-hydroxyvalerate copolymers at different concentrations (8, 14, and 22%), were studied by using photoacoustic and photothermal techniques. Mass diffusion coefficients were obtained for carbon dioxide and oxygen by using a gas analyzer. Specific heat capacity measurements were performed by monitoring temperature of the samples under white light illumination against time. Thermal diffusivities were determined by using the open photoacoustic cell configuration. The results were discussed considering the incorporation of hydroxyvalerate units in the poly(3-hydroxybutyrate) unit cell and were correlated with atomic force microscopy images of the upper surface of membranes. New information on transport properties of PHAs is provided.

Journal of Applied Polymer Science 97[4], 1491-1497. 2005.

P176-05 "Physical characterization of surface-modified liposomes by incorporation of gangliosides designed for immunotherapies".

Zanin, M. H. A., Torriani, I. C. L., Zollner, R. L., and Santana, M. H. A.

Surface-modified liposomes with gangliosides prolong their half life in blood stream that associated to the poor immunogenic properties of gangliosides are potentially useful for applications as immunotherapic vehicles. The physical characteristics of these biocolloids play an important role on their stability and exposition of the ganglioside antigens to the immunological system. The present work describes the physical characterization of liposomes incorporating a monosialoganglioside or a mixture of mono-, di- and trisialogangliosides. The liposomal matrix was composed of either dipalmitoylphosphatidylcholine and cholesterol, or in some preparations dihexadecylphosphate, which was added in order to provide a higher negative charge density on the liposome surface. Both types of liposomes were prepared by the dry phospholipids film hydration method and characterized by their phospholipid and ganglioside content, mean diameter, size distribution, morphology, membrane packing, lamellar structure and phase transition behavior.

Colloids and Surfaces A-Physicochemical and Engineering Aspects 251[1-3], 175-182. 2004.

P177-05 "Polarization effects in the elastic scattering of low-energy electrons by C3H4 isomers".

Sanchez, S. D., Lopes, A. R., Bettega, M. H. F., Lima, M. A. P., and Ferreira, L. G

In this paper we present integral and differential cross sections for electron scattering by the C3H4 isomers allene and propyne for energies from 1 to 10 eV. To compute the scattering cross sections we employ the Schwinger multichannel method with pseudopotential at the static exchange plus polarization approximation. Our results are in good agreement with experimental total cross sections and differential cross sections. We also discuss the role of the isomer effect in the cross sections of these isomers in the 1-10 eV energy range.

Physical Review A 71[6]. 062702. 2005.

P178-05 "Possible Fulde-Ferrell-Larkin-Ovchinnikov inhomogeneous superconducting state in CeCoIn5".

Movshovich, R., Bianchi, A., Capan, C., Pagliuso, P. G., and Sarrao, J. L.

We report specific heat and thermal conductivity measurements of the heavy fermion superconductor CeCoIn5 in the vicinity of the superconducting critical field H-c2, with magnetic field in the plane of this quasi-2D compound and at temperatures down to 50 mK. The superconducting phase transition changes from second to first order for field above 10T, as evident from a sharp peak in specific heat and a jump in thermal conductivity, indicating the importance of the Pauli limiting effect in CeCoIn5. In the same range of magnetic field, we observe a second specific beat anomaly within the superconducting state. We interpret this anomaly as a signature of a Fulde-Ferrell-Larkin-Ovchinnikov (FFLO) inhomogeneous superconducting state. In addition, the thermal conductivity data as a function of field display a kink at a field H-k below the superconducting critical field, which closely coincides with the low-temperature anomaly in specific heat, tentatively identified with the appearance of the FFLO superconducting state. Our results indicate that the thermal conductivity is enhanced within the FFLO state, and call for further theoretical investigations of the real-space structure of the order parameter (and in particular, the structure of vortices) and of the thermal transport within the inhomogeneous FFLO state.

Physical Review Letters 91[18]. 187004-1-187004-4. 2005.

P179-05 "Radon surveys in Brazil using CR-39".

Paulo, S. R., Neman, R., Neto, J. C. H., Iunes, P. J., Guedes, S., Balan, A. M. O. A., and Tello, C. A. S.

In this work results of two radon daughters survey in Brazil are presented and discussed. Some methodological problems concerning the first survey are pointed out which were corrected for the second survey in order to make a realistic long-term measurement of radon decay products in the air. The technique employed in both surveys was the alpha-spectroscopy using CR-39. The reliability of this technique as well as the results of the second survey are discussed, which indicate a poor correlation between radon and its decay products in the air at the researched dwellings.

Radiation Measurements 39[6], 657-660. 2005.

P180-05 "Resistive plates carrying a steady current: Electric potential and surface charges close to the battery".

Hernandes, J. A., de Oliveira, E. C., and Assis, A. K. T.

We treat the problem of two resistive plates carrying a steady current in the same direction. We consider a linear battery orthogonal to the direction of the current in the middle of the plates. We study the behavior of the surface charges close to the battery. We calculate the potential and electric field in the space outside the plates. We also consider the case of a single resistive plate carrying a steady current.

Foundations of Physics Letters 18[3], 275-289. 2005.

P181-05 "Resonant helical deformations in nonhomogeneous Kirchhoff filaments".

da Fonseca, A. F., Malta, C. P., and de Aguiar, M. A. M.

We study the three-dimensional static configurations of nonhomogeneous Kirchhoff filaments with periodically varying Young's modulus. We analyze the effects of the Young's modulus frequency and amplitude of variation in terms of stroboscopic maps, and in the regular (non chaotic) spatial configurations of the filaments. Our analysis shows that the tridimensional conformations of long filaments may depend critically on the Young's modulus frequency in case of resonance with other natural frequencies of the filament. As expected, far from resonance the shape of the solutions remain very close to that of the homogeneous case. In the case of biomolecules, although various other elements, besides sequence-dependent effects, combine to determine their conformation, our results show that sequence-dependent effects alone may have a significant influence on the shape of these molecules, including DNA.

Physica A-Statistical Mechanics and Its Applications 352[2-4], 547-557. 2005.

P182-05 "Round table discussion: Present and future applications of nanocrystalline magnetic materials".

Herzer, G., Vazquez, M., Knobel, M., Zhukov, A., Reininger, T., Davies, H. A., Grossinger, R., and Li, J. L. S.

Examples of existing or potential applications of nanocrystalline magnetic materials, ranging from soft to hard magnetic alloys, are presented and discussed by experts in the respective fields of research and technology.

Journal of Magnetism and Magnetic Materials 294[2], 252-266. 2005.

P183-05 "Semiclassical propagation of wavepackets with complex and real trajectories".

de Aguiar, M. A. M., Baranger, M., Jaubert, L., Parisio, F., and Ribeiro, A. D.

We consider a semiclassical approximation, first derived by Heller and coworkers, for the time evolution of an originally Gaussian wave packet in terms of complex trajectories. We also derive additional approximations replacing the complex trajectories by real ones. These yield three different semiclassical formulae involving different real trajectories. One of these formulae is Heller's thawed Gaussian approximation. The other approximations are non-Gaussian and may involve several trajectories determined by mixed initial-final conditions. These different formulae are tested for the cases of scattering by a hard wall, scattering by an attractive Gaussian potential and bound motion in a quartic oscillator. The formula with complex trajectories gives good results in all cases. The non-Gaussian approximations with real trajectories work well in some cases, whereas the thawed Gaussian works only in very simple situations

Journal of Physics A-Mathematical and General 38[21], 4645-4664. 2005.

P184-05 "Simulation of the fluorescence detector of the Pierre Auger Observatory".

Prado, L., Dawson, B. R., Petrera, S., Shellard, R. C., do Amaral, M. G., Caruso, R., Sato, R., and Bellido, J. A.

We present a description of a simulation program for the fluorescence detector (FD) of the Pierre Auger Observatory. The simulation chain covers in detail all the physical processes involved in the fluorescence technique, from the shower longitudinal profile in the atmosphere to ADC-traces in the data acquisition system of the telescopes. Steps in the simulation include the generation of fluorescence and Cherenkov light in the atmosphere, propagation of this light to the telescope aperture, ray-tracing of photons in the Schmidt optics of the telescopes, and finally, simulation of the response of the electronics and the multi-level trigger. As an example of the simulation's use we show the results of a calculation of the trigger efficiency of the FD as a function of cosmic ray energy.

Nuclear Instruments & Methods in Physics Research Section A-Accelerators Spectrometers Detectors and Associated Equipment 545[3], 632-642. 2005.

P185-05 "Solid-state nuclear magnetic resonance study of relaxation processes in MEH-PPV".

Bloise, A. C., DeAzevedo, E. R., Cossiello, R. F., Bianchi, R. F., Balogh, D. T., Faria, R. M., Atvars, T. D. Z., and Bonagamba, T. J.

Solid-state nuclear magnetic resonance methods were used to study molecular dynamics of MEH-PPV at different frequency ranges varying from 1 Hz to 100 MHz. The results showed that in the 213 to 323 K temperature range, the motion in the polymer backbone is predominantly slow (Hz-kHz) involving small angle librations, which occurs with a distribution of correlation times. In the side chain, two motional regimes were identified: Intermediate regime motion (1-50 kHz) for all chemical groups and, additionally, fast rotation (similar to 100 MHz) for the terminal CH3 group. A correlation between the motional parameters and the photoluminescent behaviors as a function of temperature was observed and is discussed.

Physical Review B 71[17]. 174202. 2005.

P186-05 "Solid state Pomeranchuk effect".

Continentino, M. A., Ferreira, A. S., Pagliuso, P. G., Rettori, C., and Sarrao, J. L.

Recently, we have shown that YbInCu4 and related compounds present a solid state Pomeranchuk effect. These systems have a first-order volume transition where a local moment phase coexists with a renormalized Fermi liquid in analogy with 3 He at its melting curve. We demonstrate here experimentally that the solid state Pomeranchuk effect, controlled by a magnetic field, can be used to produce cooling.

Physica B-Condensed Matter 359, 744-746. 2005.

P187-05 "Spectroscopic, electrochemical, and microgravimetric studies on palladium phthalocyanine films".

Gaffo, L., Goncalves, D., Faria, R. C., Moreira, W. C., and Oliveira, O. N.

The optical properties of palladium phthalocyanine in dimethylformamide, toluene, acetonitrile, and dichloromethane solutions were studied in the visible range of energy. Palladium phthalocyanine in organic medium presented itself as a mixture of monomeric and dimeric species in equilibrium, and it was only in dichloromethane that the monomeric, non-aggregated form predominated. Palladium phthalocyanine films were prepared by casting, and studied by cyclic voltammetry and spectroelectrochemistry. The films showed an electrochromic response from blue to purple, and stability that depended on the applied potential. Electrochemical quartz crystal microbalance experiments indicated that the film exfoliates into solution after applying high values of final potentials. Raman spectroscopy was used to structurally characterize the palladium phthalocyanine film, which showed a central metal with +2 oxidation state that is not affected even when the film is oxidized.

Journal of Porphyrins and Phthalocyanines 9[1], 16-21. 2005.

P188-05 "Structural modifications and corrosion behavior of martensitic stainless steel nitrided by plasma immersion ion implantation".

Figueroa, C. A., Alvarez, F., Zhang, Z., Collins, G. A., and Short, K. T.

In this work we report a study of the structural modifications and corrosion behavior of martensitic stainless steels (MSS) nitrided by plasma immersion ion implantation (PI3). The samples were characterized by x-ray diffraction, scanning electron microscopy, energy dispersive x-ray spectroscopy, photoemission electron spectroscopy, and potentiodynamic electrochemical measurements. Depending on the PI3 treatment temperature, three different material property trends are observed. At lower implantation temperatures (e.g., 360 degrees C), the material corrosion resistance is improved and a compact phase of epsilon-(Fe,Cr)(3)N, without changes in the crystal morphology, is obtained. At intermediate temperatures (e.g., 430 degrees C), CrN precipitates form principally at grain boundaries, leading to a degradation in the corrosion resistance compared to the original MSS material. At higher temperatures (e.g., 500 degrees C), the relatively great mobility of the nitrogen and chromium in the matrix induced random precipitates of CrN, transforming the original martensitic phase into alpha-Fe (ferrite), and causing a further degradation in the corrosion resistance.

Journal of Vacuum Science & Technology A 23[4], 693-698. 2005.

P189-05 "Structural, magnetic and transport properties of discontinuous granular multi-layers".

Denardin, J. C., Knobel, M., Dorneles, L. S., and Schelp, L. F.

Results of structural, magnetic and transport properties of magnetic Co/SiO2 discontinuous multi-layers produced by sequential deposition are presented. Transmission electron microscopy (TEM) images show that the samples that are close to metal-insulation transition are composed by a connected network of metallic paths, and display an enhanced Hall Effect. The granular samples are composed by an almost periodic array of Co nanoparticles, and after annealing these samples show a clear evolution in the nanostructure, with increasing average Co grain sizes and decreasing size dispersion. Relationships between the nanostructure and magnetotransport properties are discussed and compared with previous results obtained in cosputtered films.

Journal of Magnetism and Magnetic Materials 294[2], 206-212. 2005.

P190-05 "Studies of electrical resistivity under pressure on superconducting Sn-doped CeCoIn5".

Ramos, S. M., Fontes, M. B., Alvarenga, A. D., Baggio-Saitovitch, E., Pagliuso, P. G., Bauer, E. D., Thompson, J. D., Sarrao, J. L., and Continentino, M. A.

Experiments of electrical resistivity as a function of hydrostatic pressure for single crystals of Sn-doped CeCoIn5 are reported. Due to the subtle Sn-cloping, T, is strongly suppressed from T-c = 2.3 K of undoped CeCoIn5 to T-c similar to 0.7 K for the reported concentration (x similar to 0.12). As for pure CeCoIn5, superconductivity (SC) seems to evolve out of a non-Fermi liquid (NFL) normal state just above Tc. A temperature-pressure phase diagram is constructed from our results and compared with the properties of pure CeCoIn5 under pressure. Effects of chemical pressure and/or hybridization tuning associated with Sn-doping are discussed.

Physica B-Condensed Matter 359, 398-400. 2005.

P191-05 "Sunscreen effects in skin analyzed by photoacoustic spectroscopy".

dos Anjos, F. H., Rompe, P. C. B., Mansanares, A. M., da Silva, E. C., Acosta-Avalos, D., and Barja, P. R.

In this work, photoacoustic spectroscopy (PAS) was employed to characterize samples of commercially available sunscreen (SPF15) and the system formed by sunscreen plus skin (topically applied sunscreen). Measurements were performed at 70Hz, in the wavelength range that corresponds to most of the ultraviolet (UV) radiation that reaches Earth. The absorption spectrum of sunscreen was obtained in vitro and in situ., showing that the sunscreen analyzed presents an effective absorption of the UV radiation After that, the PAS technique was used to monitor the absorption kinetics of sunscreen applied to human skin (abdomen) samples, characterizing alterations in the human skin after application of sunscreen. This was done by applying the sunscreen in a skin sample and recording the absorption spectra in regular time intervals, up to 90 minutes after application. Measurements show that light absorption by the system sunscreen plus skin stabilizes between 25 and 45 minutes after sunscreen application. This agrees with the instructions given by the producers about the need of applying the sunscreen at least 30 minutes before sun exposition. The requirement to periodically reapply the sunscreen is confirmed by the progressive decrease in the level of UV absorption as a function of time.

Journal de Physique IV (Proceedings) 125[1], 797-799. 2005.

P192-05 "Synthesis of In2O3 nanoparticles by thermal decomposition of a citrate gel precursor".

Rey, J. F. Q., Plivelic, T. S., Rocha, R. A., Tadokoro, S. K., Torriani, I., and Muccillo, E. N. S.

This paper describes the synthesis of indium oxide by a modified sol-gel method, and the study of thermal decomposition of the metal complex in air. The characterization of the intermediate as well as the final

compounds was carried out by thermogravimetry, differential thermal analysis, Fourier transform infrared spectroscopy, X-ray diffraction, transmission electron microscopy, and small angle X-ray scattering. The results show that the indium complex decomposes to In2O3 with the formation of an intermediate compound. Nanoparticles of cubic In2O3 with crystallite sizes in the nanosize range were formed after calcination at temperatures up to 900 degrees C. Calcined materials are characterized by a polydisperse distribution of spherical particles with sharp and smooth surfaces.

Journal of Nanoparticle Research 7[2], 203-208. 2005.

P193-05 "Telegraphy equation from Weber's electrodynamics".

Assis, A. K. T. and Hernandes, J. A.

We derive the telegraphy equation according to Weber's electrodynamics for signal propagating along a very long bidimensional wire in the shape of a rectangular strip of zero thickness. We also derive this equation for a twin lead composed by two of these parallel very long bidimensional wires facing each other. We compare this result with classical electromagnetism.

Ieee Transactions on Circuits and Systems Ii-Express Briefs 52[6], 289-292. 2005.

P194-05 "Tellurite glass photonic crystal fibre amplifier".

Osorio, S. P. A., Chilcce, E. F., Rodriguez, E., Cesar, C. L., and Barbosa, L. C.

The fabrication and characterisation of a tellurite photonic crystal fibre amplifier is reported. The preform consists of a 12 mm external diameter tellurite tube which is filled with an array of nonperiodic tellurite capillaries and an erbium doped tellurite rod that constitutes the fibre nucleus. The preform was drawn in a Heathway Drawing Tower, producing fibres with diameters between 120-140 pm. Cross sections of the fibre photographed in an optical microscope shows that the light is being guided by total internal reflection. The following characteristics of the fibre were assessed: photoluminescence, refractive index, absorbance, thermal properties and spontaneous emission spectra.

Glass Technology - European Journal of Glass Science and Technology Part A 46[2], 160-162. 2005.

P195-05 "Terahertz excitation and coherence effects of two-level donor systems in GaAs quantum dots".

Brandi, H. S., Latge, A., and Oliveira, L. E.

The confinement effects on the electronic and donor states in GaAs-(Ga, Al)As quantum dots, in the presence of an applied magnetic field, are studied. Using the optical Bloch equations with damping, we study the time evolution of the 1s, 2p_, and 2p(+), states in the presence of an applied magnetic field and of a terahertz laser. We discuss the conditions to obtain a bound 2p(+) state in contrast to the bulk situation, where the 2p(+) state is resonant with the continuum states (in this case, decoherence may be a serious problem for practical realizations). We show that the pronounced confining effects of semiconductor quantum dots lead to conditions such that the 2p(+) excited donor state may lie below the continuum, originating a favourable situation concerning the coherence time of the corresponding Rabi oscillations. We also calculate the electric dipole transition moment, discuss the photosignal, and the possible experimental conditions under which decoherence is weak and qubit operations are efficiently controlled.

Journal of Physics-Condensed Matter 17[23], 3665-3671. 2005.

P196-05 "The Brazilian gravitational wave detector Mario Schenberg: progress and plans".

Aguiar, O. D., Andrade, L. A., Barroso, J. J., Bortoli, F., Carneiro, L. A., Castro, P. J., Costa, C. A., Costa, K. M. F., de Araujo, J. C. N., de Lucena, A. U., de Paula, W., Netol, E. C. D., de Souza, S. T., Fauth, A. C., Frajuca, C., Frossati, G., Furtado, S. R., Magalhaes, N. S., Marinho, R. M., Matos, E. S., Melo, J. L., Miranda, O. D., Oliveira, N. F., Paleo, B. W., Remy, M., Ribeiro, K. L., Stellati, C., Velloso, W. F., and Weber, J.

The Schenberg gravitational wave detector is almost completed for operation at its site in the Physics Institute of the University of Sao Paulo, under the full support of FAPESP (the Sao Paulo State Foundation for Research Support). We have been working on the development of a transducer system, which will be installed after the arrival of all the microwave components and the completion of the transducer mechanical parts. The initial plan is to operate a CuA16% two-mode parametric transducer in a first operational run at 4.2 K with nine transducers and an initial target sensitivity of h similar to 2 x 10(-21) Hz(-1/2) in a 50 Hz bandwidth around 3.2 kHz. Here we present details of this plan and some recent results of the development of this project

Classical and Quantum Gravity 22[10], S209-S214. 2005.

P197-05 "The dynamics of excitons and trions in resonant tunneling diodes".

Camps, I., Makler, S. S., Vercik, A., Gobato, Y. G., Marques, G. E., and Brasil, M. J. S. P.

The aim of this work is to study the dynamic formation and dissociation of trions and excitons in double barrier resonant tunneling diodes. We propose a system of rate equations that takes into account the formation, dissociation and annihilation of these complexes inside the quantum well. From the solutions of the coupled equations, we are able to study the modulation of excitons and trions formation in the device as a function of the applied bias. The results of our model agree qualitatively with the experiments showing the viability of these rate equations system to study the dynamics of complex systems.

Solid State Communications 135[4], 241-246. 2005.

P198-05 "The effect of cyclic voltammetry on the crystalline order of PdPc thin films".

Gaffo, L., Brasil, M. J. S. P., Cerdeira, F., Giles, C., and Moreira, W. C.

The degree of crystalline order of evaporated and cast palladium phthalocyanine films was investigated before and after they were submitted to a voltammetric process. X-ray diffraction and UV-vis spectroscopy measurements demonstrated that the electrochemical treatment improves the crystalline quality of the films. The X-ray results revealed an increase of the average size of the crystallites composing the films as well as a decrease in the spacing between the lattice planes in the direction perpendicular to the surface of the film. Optical measurements showed that the electrochemical treatment also introduces an appreciable degree of in-plane ordering. These improvements of crystalline order are observed in both types of films, cast and evaporated, which indicates that the ordering is a direct consequence of the electrochemical treatment and not of the method used for the film deposition.

Journal of Porphyrins and Phthalocyanines 9[2], 89-93. 2005.

P199-05 "The magnetic and magnetocaloric properties of Gd5Ge2Si2 compound under hydrostatic pressure".

Carvalho, A. M. G., Alves, C. S., de Campos, A., Coelho, A. A., Gama, S., Gandra, F. C. G., von Ranke, P. J., and Oliveira, N. A.

The Gd5Ge2Si2 compound presents a giant magnetocaloric effect with transition temperature at around 276 K and is a very good candidate for application as an active regenerator material in room temperature magnetic refrigerators. Recently it has been shown that pressure induces a colossal magnetocaloric effect in MnAs, a material that presents a giant magnetocaloric effect and a strong magnetoelastic coupling, as also happens with the Gd5Ge2Si2 compound. This motivated a search of the colossal effect in the Gd5Ge2Si2 compound. This work reports our measurements on the magnetic properties and the magnetocaloric effect of Gd5Ge2Si2 under hydrostatic pressures up to 9.2 kbar and as a function of temperature. Contrary to what happens with MnAs, pressure increases the Curie temperature of the compound, does not affect the saturation magnetization and decreases markedly its magnetocaloric effect.

Journal of Applied Physics 97[10]. 10M320-10M320-3. 2005.

P200-05 "The use of apatite fission track thermochronology to constrain fault movements and sedimentary basin evolution in northeastern Brazil".

da Nobrega, M. A., Sa, J. M., Bezerra, F. H. R., Neto, J. C. H., Iunes, P. J., Guedes, S., Saenz, C. A. T., Hackspacher, P. C., and Lima-Filho, R.

An apatite fission track study of crystalline rocks underlying sedimentary basins in northeastern Brazil indicate that crustal blocks that occur on opposite sides of a geological fault experienced different thermal histories. Samples collected on the West block yielded corrected fission-track ages from 140 to 375 Ma, whereas samples collected on the East block yielded ages between 90 and 125 Ma. The thermal models suggest that each block experienced two cooling events separated by a heating event at different times. We concluded that the West block moved downward relative to the East block ca. 140 Ma ago, when sediments eroded from the East side were deposited on the West side. This process represents the early stage of sedimentary basin formation and the opening of the South Atlantic Ocean in the region. Downward and upward movements related to heating and cooling events of these crustal blocks at different periods until recent times are proposed.

Radiation Measurements 39[6], 627-633. 2005.

P201-05 "Thermal diffusivity and photoacoustic spectroscopy measurements in CdTe quantum dots borosilicate glasses".

da Silva, V. L., Mesquita, R. C., da Silva, E. C., Mansanares, A. M., and Barbosa, L. C.

In this paper we describe the results of photoacoustic spectroscopy and thermal diffusivity measurements in borosilicate glass matrix with CdTe quantum dots. Samples treated at the temperature of 540(0)C for different periods were studied. The photoacoustic spectra show the absorption band of CdTe quantum dots, which shifts as a function of the thermal treatment time, revealing the evolution of the average radius of the nanocrystals. Thermal lens measurements provide the thermal diffusivity of the treated samples and give the behavior of the temperature coefficient of the refractive index, dn/dT, which is correlated to the transmittance spectra.

Journal de Physique IV (Proceedings) 125[1], 273-276. 2005.

P202-05 "Thermochronology of the South American platform in the state of Sao Paulo, Brazil, through apatite fission tracks".

Saenz, C. A. T., Neto, J. C. H., Iunes, P. J., Guedes, S., Hackspacher, P. C., Ribeiro, L. F. B., Paulo, S. R., and Osorio, A. M. A.

The fission-track method (FTM) in apatite was applied to 45 samples collected in the Serra da Mantiqueira (Mantiqueira mountain range), the Serra do Mar (Mar mountain range), regions next to these mountain ranges and the coastal region between Ubatuba and Santos in the State of Sao Paulo, Brazil, to study the thermochronology of the South American Platform in southeast Brazil and its influence on Santos and Campos basins. The data presented in this work complement the previously presented data on the same region (Tello Saenz et al., 2003. J. S. Am. Earth Sci. 15, 765-774) with 31 new samples analyzed. The weighted mean of the corrected ages from high Mantiqueira (around 1000 m), (121 +/- 6) Ma, coincides with the South Atlantic opening. The fact that its thermal history starts at a relatively low temperature (similar to 80 degrees C) suggests that the age of similar to 120 Ma would be the formation age of Serra da Mantiqueira due to a rapid pulse, in which tracks had no time to be retained at the closure temperature, that is similar to 120 degrees C. The Serra do Mar presents a more complicated thermal history, with several reactivations indicated by the changes in the slope of its cooling curve. The thermal histories obtained in the regions next to these mountain ranges are compatible with the results mentioned above. The Santos Basin has unconformities that agree with changes in the slope thermal histories of the studied region.

Radiation Measurements 39[6], 635-640. 2005.

P203-05 "Thermoreflectance measurements on test microelectronic devices at several probe wavelengths: Comparison between CCD and focused laser techniques".

de Freitas, L. R., Mansanares, A. M., da Silva, E. C., Pimentel, M. C. B., Finco, S., Tessier, G., and Fournier, D.

In this paper we present thermoreflectance measurements on polycrystalline silicon conducting tracks for several wavelengths of the probe beam. Two distinct experimental setup were employed, namely, the CCD camera setup and the focused laser setup. It is shown that the thermoreflectance signal behavior is closely related to the derivative of the optical reflectance with respect to the wavelength

Journal de Physique IV (Proceedings) 125[1], 121-124. 2005.

P204-05 "Thermoreflectance microscopy applied to the study of electrostatic discharge degradation in metal-oxide-semiconductor field-effect transistors".

de Freitas, L. R., da Silva, E. C., Mansanares, A. M., Pimentel, M. B. C., Filho, S. E., and Batista, J. A.

We investigated the effect of electrostatic discharge on n-channel metal-oxide-semiconductor field-effect transistors using the thermoreflectance microscopy. The gate terminals of the transistors were submitted to electrostatic pulses on a zap system that respects the human body model. The pulse intensity varied from 40 to 140 V in a cumulative sequence. Electrical characterization showed that the transistor threshold voltage was no longer positive for pulses of 110 V and higher. No significant changes in the thermoreflectance maps were observed in these cases. For pulses of 140 V a large leakage current appeared, and the thermoreflectance maps revealed strong peaks (localized spot) associated with the induced damage.

Journal of Applied Physics 97[10]. 104510. 2005.

P205-05 "Thermotectonic and fault dynamic analysis of Precambrian basement and tectonic constraints with the Parana basin".

Ribeiro, L. R. B., Hackspacher, P. C., Ribeiro, M. C. S., Neto, J. C. H., Tello, S. C. A., Iunes, P. J., Franco, A. O. B., and Godoy, D. R.

The Precambrian crystalline basement of southeast Brazil is affected by many Phanerozoic reactivations of shear zones that developed during the end of the Neoproterozoic in the Brasiliano orogeny. These reactivations with specific tectonic events, a multidisciplinary study was done, involving geology, paleostress, and structural analysis of faults, associated with apatite fission track methods along the northeastern border of the Parana basin in southeast Brazil. The results show that the study area consists of three main tectonic domains, which record different episodes of uplift and reactivation of faults. These faults were brittle in character and resulted in multiple generations of fault products as pseudotachylytes and ultracataclasites, foliated cataclasites and fault gouges. Based on geological evidence and fission track data, an uplift of basement rocks and related tectonic subsidence with consequent deposition in the Parana basin were modeled. The reactivations of the basement record successive uplift events during the Phanerozoic dated via corrected fission track ages, at 387 +/- 50 Ma (Ordovician); 193 +/- 19 Ma (Triassic); 142 +/- 18 Ma (Jurassic), 126 +/- 11 Ma (Early Cretaceous); 89 +/- 10 Ma (Late Cretaceous) and 69 +/- 10 Ma (Late Cretaceous). These results indicate differential uplift of tectonic domains of basement units, probably related to Parana basin subsidence. Six major sedimentary units (supersequences) that have been deposited with their bounding unconformities, seem to have a close relationship with the orogenic events during the evolution of southwestern Gondwana.

Radiation Measurements 39[6], 669-673. 2005.

P206-05 "Time-dependent strain analysis of mirrors illuminated with intense femtosecond pulses in the soft x-ray spectral range".

de Castro, A. R. B. and Moller, T.

We consider the three-dimensional time-dependent thermoelastic problem for a thin silicon blade illuminated by a single soft x-ray free-electron laser (FEL) pulse of fs duration. An exact analytical solution is given. It shows that the heat flow in the blade is very slow, which might pose problems for cooling if the FEL is operated to produce a train of pulses with short spacing. Surface mechanical oscillations are generated shortly after the FEL pulse is absorbed, and resonant enhancement by subsequent pulses in the pulse train is an issue. After the FEL pulse, but long before the heat front reaches the heat sink, the optical surface bulges outwards. The effects of a FEL pulse train with thousands of pulses need more detailed study, but experiments with single pulses at kHz rates are not expected to suffer from thermally induced surface figure distortion. The emphasis in this article is not on whether the blade will escape melting, but rather to what extent the profile of a high precision optical surface is preserved under FEL illumination, a question of major interest if focal spots with diameters in the micron range are needed.

Review of Scientific Instruments 76[6]. 063104-063104-6. 2005.

P207-05 "U and Th thin film neutron dosimetry for fission-track dating: application to the age standard Moldavite".

Iunes, P. J., Bigazzi, G., Neto, J. C. H., Laurenzi, M. A., Balestrieri, M. L., Norelli, P., Araya, A. M. O., Guedes, S., Tello, C. A. S., Paulo, S. R., Moreira, P. A. F. P., Palissari, R., and Curvo, E. A. C.

Neutron dosimetry based on U and Th thin films was used for fission-track dating of the age standard Moldavite, the central European tektite, from the Middle Miocene deposit of Jankov (southern Bohemia, Czech Republic). Our fission-track age (13.98 +/- 0.58 Ma) agrees with a recent Ar-40/Ar-39 age, 14.34 +/- 0.04 Ma, based on several determinations on Moldavites from different sediments, including the Jankov deposit. This result indicates that the U and Th thin film neutron dosimetry represents a reliable alternative for an absolute approach in fission-track dating.

Radiation Measurements 39[6], 665-668. 2005.

P208-05 "Uncooled performance of 10-Gb/s laser modules with InGaAlAs-InP and InGaAsP-InP MQW electroabsorption modulators integrated with semiconductor amplifiers".

Frateschi, N. C., Zhang, J., Jambunathan, R., Choi, W. J., Ebert, C., and Bond, A. E.

Uncooled operation of long-reach high performance C-band 10 Gb/s of optical modulator modules is presented. Modules consisting of a distributed feedback laser and a chip with a monolithically integrated electroalisorption modulator and semiconductor optical amplifier based on multiquantum-well structures of both InGaAsP-InP and InGaAlAS-InP material systems are presented. Dispersion penalty of 1 dB over 94-km transmission, output power above 0 dBm, and low extinction ratio variation are demonstrated over an 80 degrees C temperature range. A simple analysis of the quantum confined Stark effect is employed to explain the temperature-dc bias voltage dependence.

IEEE Photonics Technology Letters 17[7], 1378-1380. 2005.

Nota: Arquivo gerado em 06/2012, a partir da página web, pois o original não foi preservado.

Abstracta

Instituto de Física
Diretor: Prof. Dr. Júlio Cesar Hadler Neto
Universidade Estadual de Campinas - UNICAMP
Cidade Universitária C.P. 6165
CEP: 13081-970 - Campinas - SP - Brasil
e-mail: secdir@ifi.unicamp.br
Fone: 0XX 19 3521-5300

Publicação

Biblioteca do Instituto de Física Gleb Wataghin
http://webbif.ifi.unicamp.br
Diretora Técnica: Rita Aparecida Sponchiado

Elaboração
Tânia Macedo Folegatti
absctact@ifi.unicamp.br

Projeto Gráfico
ÍgneaDesign

Impressão

Gráfica Central - Unicamp